Proton–donor properties of water and ammonia in van der Waals complexes with rare-gas atoms. Kr–H_2O and Kr–NH_3

G. Chałasiński
Department of Chemistry and Biochemistry, Southern Illinois University, Carbondale, Illinois 62901, and Department of Chemistry, Oakland University, Rochester, Michigan 48309, and Department of Chemistry, University of Warsaw, Pasteura 1, 02-093 Warszawa, Poland[a)]

M. M. Szczęśniak
Department of Chemistry, Oakland University, Rochester, Michigan 48309

S. Scheiner
Department of Chemistry and Biochemistry, Southern Illinois University, Carbondale, Illinois 62901

(Received 22 June 1992; accepted 20 August 1992)

The perturbation theory of intermolecular forces in conjunction with the supermolecular Møller–Plesset perturbation theory is applied to the analysis of the potential-energy surfaces of Kr–H_2O and Kr–NH_3 complexes. The valleylike minimum region on the potential-energy surface of Kr–H_2O ranges from the coplanar geometry with the C_2 axis of H_2O nearly perpendicular to the O–Kr axis (T structure) to the H-bond structure in which Kr faces the H atom of H_2O. Compared to the previously studied Ar–H_2O [J. Chem. Phys. **94**, 2807 (1991)] the minimum has more of the H-bond character. The minimum for Kr–NH_3 corresponds to the T structure only, in accordance to the result for Ar–NH_3 [J. Chem. Phys. **91**, 7809 (1989)]. The minima in Kr–H_2O and Kr–NH_3 are roughly 27% and 19%, respectively, deeper than for the analogous Ar complexes. To examine the proton–donor abilities of O–H and N–H bonds the ratios of the deformation energy to dispersion energy are considered. They reflect fundamental differences between the two bonds and explain why NH_3 is not capable of forming the H-bond structures to rare-gas atoms.

I. INTRODUCTION

Conventional wisdom about the hydrogen bond suggests that water and ammonia should have basically similar hydrogen-bonding capabilities. That is, both should be able to act as a hydrogen-bond donor and as a hydrogen-bond acceptor. However, while this is true for the water molecule, there is no known example of the ammonia molecule acting as a proton donor in the gas phase. More specifically, the high-resolution gas-phase spectroscopic studies of a number of van der Waals complexes involving ammonia in no instance detected angular expectation values or vibrationally averaged structures which would indicate that NH_3 acted as a proton donor, (see recent discussions by Schmuttenmaer *et al.*[1] and Suni, Lee, and Klemperer[2]). Perhaps the only exception will turn out to be the ammonia dimer where the inversion of vibration–rotation–tunneling (V–T–R) spectra recently revealed a broad minimum encompassing both the cyclic and H-bonded structures,[3] in contrast to the previous studies which pointed to the cyclic (i.e., non-H-bonded) structure only.[4]

These anomalous properties of ammonia provide the chemical motivation for the present study. Studies of proton–donor properties are important in a broader context for understanding the nature of the hydrogen bond. In particular, the following issues should be addressed: What is so peculiar about the potential-energy surface (PES) in the region where one of the protons of the ammonia molecule contacts other atoms and molecules, and how does this contact differ from that of the water's proton? It is particularly interesting whether these differences are reflected in the individual contributions to the interaction energy, such as the electrostatic, exchange, induction, and dispersion, and whether they can be related to any of the monomer properties. Such an analysis will help predict whether it is possible to find a complex where NH_3 acts as a proton donor.

A great deal of experimental effort has been devoted recently to the systematic investigation of the weak bonding properties of NH_3 by using the Ar atom as a structureless probe.[1,5–7] There have also been several *ab initio* efforts towards the characterization of the Ar–NH_3 complex.[8–10] Both experimental and theoretical studies indicate that NH_3 avoids the hydrogen-bonded structure with a reasonably strong Lewis base, such as Ar. At the same time there have been a number of quite ingenious attempts at finding a strong proton acceptor, preferably with simple geometry, to which NH_3 would form a donor hydrogen bond.[2]

Our previous studies of a number of complexes formed by Ar and various hydrides, such as Ar–NH_3,[8] Ar–H_2O,[11] Ar–CH_4,[12] and Ar–HCl[13] (see also Ref. 14), seem to indicate that the ability to form a H-bonded structure is related to the self-consistent-field (SCF) deformation (or induction) energy. The induction energy depends upon two factors: high polarizability of the rare-gas atom and the strength of the electric field along the X–H bond in the hydride. For example, in the Rg–HX (X=F, Cl, Br) complexes the global minimum usually occurs for the H-bond

[a)]Permanent address.

geometry Rg–H-X.[15] The only exception found is He–HBr, which combines the least polar HBr with the least polarizable He. Furthermore, the secondary minimum for the Ar–HX complexes (Ar–X-H) is the closer in energy to the primary minimum the lower the dipole moment of HX.[15]

The Rg–H_2X complexes are also consistent with this picture. In Ar–H_2O a broad minimum encompasses both the H-bond geometry and the (coplanar) T-shaped structure with almost perpendicular arrangement of the C_2–water axis and the Ar–O axis.[11,16] Ar–H_2S (Ref. 17) and He–H_2O,[18] on the other hand, reveal coplanar *T* structures only. Both H_2S and He are less polar and less polarizable, respectively, than H_2O and Ar.

In the Rg–H_3X van der Waals systems, as mentioned above, no H-bonded structures have been found yet. In search for a likely candidate we turn to the Kr atom which, by virtue of its high polarizability, appears to be more likely than Ar to form a complex involving the H-bond structure with ammonia. In the present paper, *ab initio* studies of Kr–NH_3 and Kr–H_2O are reported. It is anticipated that the comparison of these two systems, along with their Ar analogs, Ar–NH_3 and Ar–H_2O, will shed new light on the nature of the H bond.

The study will be carried out within the framework of the perturbation theory of intermolecular forces[19] combined with the supermolecular Møller–Plesset perturbation theory.[20,21] This approach provides, in a consistent manner, all the contributions to the interaction energy along with the total PES, and it has proven quite successful in the analysis of a number of Ar–molecule complexes.[8,11–13]

II. METHOD AND DEFINITIONS

The supermolecular Møller–Plesset perturbation theory (MPPT) interaction energy corrections are derived as the difference between the values for the total energy of the dimer and the sum of the subsystem energies, in every order of perturbation theory

$$\Delta E^{(n)} = E_{AB}^{(n)} - E_A^{(n)} - E_B^{(n)}, \quad n = \text{SCF},2,3,4,\ldots . \tag{1}$$

The sum of corrections through the *n*th order will be denoted $\Delta E(n)$; thus, e.g., $\Delta E(3)$ will symbolize the sum of ΔE^{SCF}, $\Delta E^{(2)}$, and $\Delta E^{(3)}$. Each individual $\Delta E^{(n)}$ correction can be interpreted[20] in terms of intermolecular Møller–Plesset perturbation theory (IMPPT) which encompasses all well-defined and meaningful contributions to the interaction energy such as electrostatic, induction, dispersion, and exchange, and may be expressed in the form of a double perturbation expansion.[19] The IMPPT interaction energy corrections are denoted $\epsilon^{(ij)}$, where *i* and *j* refer to the order of the intermolecular interaction operator and the intramolecular correlation operator, respectively (see Ref. 19 for more details).

A. Partitioning of ΔE^{SCF}

ΔE^{SCF} can be dissected as follows (cf. Refs. 20 and 21 for more details)

$$\Delta E^{\text{SCF}} = \Delta E^{\text{HL}} + \Delta E_{\text{def}}^{\text{SCF}}, \tag{2}$$

$$\Delta E^{\text{HL}} = \epsilon_{\text{es}}^{(10)} + \epsilon_{\text{exch}}^{\text{HL}}, \tag{3}$$

where ΔE^{HL} and $\Delta E_{\text{def}}^{\text{SCF}}$ are the Heitler–London and SCF-deformation contributions, respectively. ΔE^{HL} is further divided into the electrostatic $\epsilon_{\text{es}}^{(10)}$ and exchange $\epsilon_{\text{exch}}^{\text{HL}}$ components. The SCF deformation originates from mutual electric polarization restrained by the Pauli (antisymmetry) principle.[22,23]

B. Partitioning of $\Delta E^{(2)}$

$$\Delta E^{(2)} = \epsilon_{\text{es},r}^{(12)} + \epsilon_{\text{disp}}^{(20)} + \Delta E_{\text{def}}^{(2)} + \Delta E_{\text{exch}}^{(2)}. \tag{4}$$

$\epsilon_{\text{es},r}^{(12)}$ denotes the second-order electrostatic correlation energy with response effects,[21] and $\epsilon_{\text{disp}}^{(20)}$ the Hartree–Fock dispersion energy. $\Delta E_{\text{def}}^{(2)}$ and $\Delta E_{\text{exch}}^{(2)}$ stand for the second-order deformation correlation correction to the SCF deformation and the second-order exchange correlation, respectively. The latter encompasses the exchange-correlation effects related to electrostatic correlation and dispersion and can be approximated as follows[8,21] (provided the deformation-correlation contribution is negligible):

$$\Delta E_{\text{exch}}^{(2)} = \Delta E^{(2)} - \epsilon_{\text{disp}}^{(20)} - \epsilon_{\text{es},r}^{(12)}. \tag{5}$$

C. Calculations of interaction energies

Unless stated otherwise, calculations of all the supermolecular and perturbational interaction terms are performed using the basis set of the entire complex, i.e., dimer-centered basis sets (DCBS).[24–28] This procedure amounts to applying the counterpoise method of Boys and Bernardi.[29] To assure the consistency of evaluation of the MPPT and IMPPT interaction energy corrections all the intermolecular perturbation terms $\epsilon^{(ij)}$ must be derived in DCBS as well.[30]

D. Basis sets and geometries

Medium-size polarized basis sets of Sadlej[31] (10*s*6*p*4*d*/5*s*4*p*) contracted to [5*s*3*p*2*d*/3*s*2*p*] were used for H_2O and NH_3. The krypton atom has been described by the well-tempered basis set of Huzinaga, Kłobukowski, and Tatewaki[32] (16*s*13*p*10*d*) contracted to (9*s*6*p*4*d*). The exponents and coefficients, except for the two most diffuse *d* orbitals, were taken from Ref. 32, whereas the two most diffuse *d* orbitals were optimized by Andzelm *et al.*[33] The Kr basis set which is referred to as the *spd* basis is shown in Table I.

The calculations were carried out using GAUSSIAN 88 (Ref. 34) and 90 (Ref. 35) programs and the intermolecular perturbation theory package of Cybulski.[36]

The geometrical parameters of Kr–H_2O and Kr–NH_3 complexes are defined in Fig. 1. The scan of the potential-energy surface was limited to the vicinity of the van der Waals minimum. Therefore, only the coplanar motion of the Kr atom around water was considered; see Fig. 1(a). The out-of-plane Rg motions were found to increase the energy in the case of previously studied Ar–H_2O complex.[11] In the case of Kr–NH_3 two scans of the PES were particularly interesting $\chi = 0°$ and $\chi = 60°$. In the former

TABLE I. Basis set for krypton. Exponents are in a_0^{-2}. The SCF energy is −2752.038 558 87 hartrees, and the second-order MP (MP2) correction (the range of frozen core is 1–10) is −0.158 567 803 82 hartrees.

		Coefficients		
	Exponents	1*s*	2*s*	3*s*
1*s*, 2*s*, 3*s*	826 606.45	0.000 149	0.000 019	0.000 006
	131 163.09	0.001 119	0.000 141	0.000 045
	29 210.966	0.006 092	0.000 773	0.000 247
	8156.7678	0.025 257	0.003 254	0.001 036
	2649.7239	0.084 443	0.011 340	0.003 621
	960.448 68	0.220 612	0.032 949	0.010 507
	372.570 14	0.401 754	0.077 095	0.024 815
	150.827 64	0.343 918	0.107 866	0.034 780
	62.134 097	0.065 070	−0.051 945	−0.016 605
	26.566 302	0.000 513	−0.515 351	−0.182 835
4*s*	11.486 045	1.0		
5*s*	4.994 1865	1.0		
6*s*	2.166 8098	1.0		
7*s*	0.854 822 73	1.0		
8*s*	0.338 96199	1.0		
9*s*	0.122 77414	1.0		

		Coefficients		
	Exponents	1*p*	2*p*	3*p*
1*p*, 2*p*, 3*p*	8156.7678	0.000 443	−0.000 180	0.000 049
	2649.7239	0.002 228	−0.000 909	0.000 248
	960.448 68	0.011 921	−0.004 906	0.001 332
	372.570 14	0.049 358	−0.020 696	0.005 661
	150.827 64	0.168 679	−0.073 665	0.020 176
	62.134 097	0.382 716	−0.178 778	0.049 679
	26.566 302	0.421 964	−0.198 351	0.054 541
	11.486 045	0.142 601	0.155 880	−0.055 839
	4.994 186 5	0.004 943	0.571 673	−0.206 760
	2.166 809 8	0.002 304	0.384 684	−0.152 423
4*p*	0.854 822 73	1.0		
5*p*	0.338 961 99	1.0		
6*p*	0.122 774 14	1.0		
1*d*	372.570 14	−0.001 570		
	150.827 64	−0.008 162		
	62.134 097	−0.040 081		
	26.566 302	−0.137 174		
	11.486 045	−0.309 108		
	4.994 186 5	−0.405 223		
	2.166 809 8	−0.301 638		
2*d*	0.854 822 73	1.0		
3*d*	0.552	1.0		
4*d*	0.150	1.0		

the Kr atom passes between two N–H bonds, and in the latter it eclipses one N–H bond. The internal geometrical parameters of H_2O and NH_3 were the following: O–H =0.9572 Å, H–O–H=104.524° and N–H=1.012 42 Å, H–N–H=106.67°.

III. RESULTS AND DISCUSSION

A. Anisotropy of interaction energies

1. Kr–H_2O

The interaction energies obtained at the MP2/*spd* level for Kr–H_2O are listed in Table II. The region around the minimum qualitatively resembles that for Ar–H_2O.[11] The region is fairly broad and Kr can move almost isoenergetically (within less than 1 cm^{-1}) from $\theta=100°$ to $\theta=120°$ at $R=7.5\ a_0$. When R is allowed to vary, the motion ranging from $\theta=60°$ at $R=7.0\ a_0$ to $\theta=120°$ at $R=8.0\ a_0$, raises the energy by less than 8.5 cm^{-1} above the minimum. In the case of the previously studied Ar–H_2O,[11] a similar path was somewhat shifted toward smaller θ angles and was flatter; the angular motion of Ar ranged from 60° at 6.61 a_0 to 120° at 7.56 a_0 corresponding to an energy increase of ca. 3 cm^{-1} above the minimum.[11] Furthermore, the minimum for Kr–H_2O is deeper and shifted toward large angles and longer distances than in the Ar–H_2O case. Indeed, for Ar–H_2O the minimum of ca. −81.7 cm^{-1} occurred at the (R,θ) values of (7.09 a_0, 80°) while for Kr–H_2O the minimum of about −103.5 cm^{-1} occurs at (7.5 a_0, 100°). It is possible to conclude that Kr more nearly approaches the H-bonded position than Ar, in agreement with our expectations based on the larger polarizability of Kr. Finally, we note that the barrier to the in-plane motion (at $\theta=0.0°$) is slightly larger in Kr–H_2O (24.7 cm^{-1}) than in Ar–H_2O (21.4 cm^{-1}). It is important to note that all the above estimates, in particular that of D_e, may be too small by some 20%–30%, primarily due to the basis-set unsaturation of the dispersion component.[8,11–13]

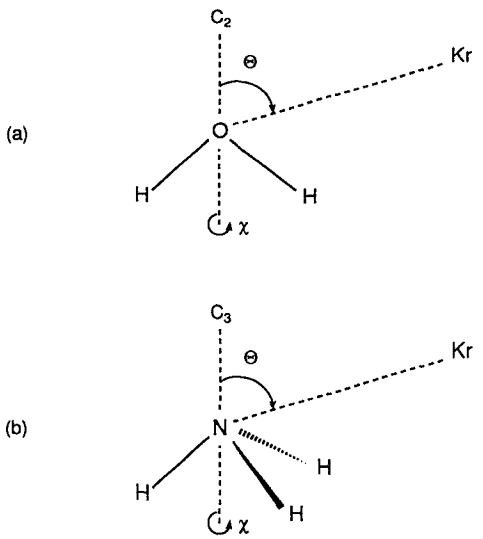

FIG. 1. Geometrical parameters of the complexes considered: (a) Kr–H_2O (Ar–H_2O); (b) Kr–NH_3 (Ar–NH_3).

Table III provides the partitioning of the interaction energies at two geometries in the region of the van der Waals minimum: the T geometry with (7.0 a_0, 80°) and the H-bond geometry with (7.5 a_0, 120°). The results qualitatively resemble those obtained for Ar–H_2O. Indeed, for both complexes, the major difference between the T and H-bond geometries is due to the substantially larger SCF-deformation (or induction) effect in the latter. It is also seen that the T geometry is favored by the dispersion and electrostatic terms, whereas the H-bond geometry is favored by the SCF-deformation term. A neglect of the SCF-deformation contribution for the H-bond geometry would qualitatively distort the shape of PES by raising substan-

TABLE II. R and θ dependence of the ΔE^{SCF} and the total $\Delta E(2)$ interaction energies for Kr–H_2O coplanar ($\chi=0°$) configuration (for definitions see the text); all energies in μhartrees.

θ	$R=7.0\ a_0$		$R=7.5\ a_0$		$R=8.0\ a_0$	
(deg)	SCF	$\Delta E(2)$	SCF	$\Delta E(2)$	SCF	$\Delta E(2)$
180	827.2	−90.9	276.5	−348.9	68.3	−360.51
160	926.0	−75.0	306.0	−367.5	74.0	−383.7
140	1073.7	−93.0	345.9	−418.5	78.9	−431.1
120	1001.1	−211.7	315.5	−468.1	68.3	−449.0
100	705.6	−360.2	222.0	−471.7	49.8	−409.9
80	430.4	−435.9	136.3	−435.4	33.3	−349.8
60	294.1	−434.0	92.5	−393.2	23.1	−306.2
40	258.8	−398.5	77.3	−366.4	15.9	−287.3
0	263.9	−359.2	71.2	−351.9	7.7	−282.8

tially the energy of the H-bonded configuration. Finally, it is worthwhile to note that the SCF-deformation effects are larger for Kr than for Ar.

2. Kr–NH_3

The values of the interaction energy obtained at the MP2 level are listed in Table IV. We first focus on the van der Waals minimum region ($R,\theta,\chi=0°$) with R ranging from 7.0 a_0 to 8.0 a_0 and θ from 0° to 180° and the region of the H-bond configuration ($R,\theta,\chi=60°$) with R ranging from 7.5 a_0 to 8.5 a_0 and θ from 0° to 180°. The van der Waals minimum for Kr–NH_3 occurs at (7.5 a_0, 80°, 0°) with $D_e=108\ \mathrm{cm}^{-1}$ and corresponds to a T configuration. Compared to Ar–NH_3 it is deeper and shifted toward larger distances, as the respective values for Ar–NH_3 are $D_e\cong 91\ \mathrm{cm}^{-1}$ and $R_e\cong 7.09\ a_0$.[8] The H-bond configuration (8.0 a_0, 100°, 60°) of Kr–NH_3 corresponds to a saddle point on the PES, some 16.5 cm^{-1} above the global minimum. It is worth reiterating that all the above estimates, in particular that of D_e, may be too small by 20%–30%, primarily due to the basis-set unsaturation of the dispersion component.[8,11–13]

One reason that Kr–NH_3 does not form a H-bonded structure is the fact that in the range of R from 7 to 8 a_0 the potential-energy surface is folded in such a way that the region between N–H bonds ($\chi=0°$) constitutes a "valley" on the PES while the region eclipsing an H atom ($\chi=60°$) is on a "ridge" (see Table IV). The origin of this pattern is the strong exchange repulsion present near the hydrogen atoms. At longer distances 9–10 a_0, however, the configuration of the surface is seen to reverse. For example, at $R=9\ a_0$ the region at $\chi=0°$ becomes less favorable than the one at $\chi=60°$ (see Table IV). Consequently, at longer distances the valley appears that leads toward an H atom of ammonia. The valley is due to the dispersion energy, which in the absence of strong exchange–repulsion dominates in this range of R. It should be emphasized that the long-range valleys leading to H atoms were first detected on the PES of Ar–NH_3 obtained by the inversion of V–T–R spectra.[37] Our result provides additional evidence that the present-day spectroscopic techniques combined with inversion methods are accurate enough to provide the finest details of the PES. Finally, we might add at this juncture that similar long-range valleys corresponding to

TABLE III. Interaction energy contributions for Kr–H_2O and Ar–H_2O in the H-bonded and T geometries. The parameters in parentheses correspond to the (R,θ) values; all energies in μhartrees.

	Kr–H_2O		Ar–H_2O	
	T (7.0 a_0, 80°)	H-bond (7.5 a_0, 120°)	T (7.09 a_0, 80°)	H-bond (7.56 a_0, 120°)
ΔE^{SCF}	430.4	315.5	156.8	111.7
$\Delta E^{(2)}$	−866.3	−783.7	−528.8	−474.7
$\Delta E(2)$	−435.9	−468.2	−372.0	−364.9
ϵ_{exch}^{HL}	837.7	797.3	323.1	341.1
$\epsilon_{es}^{(10)}$	−219.6	−171.5	−80.6	−72.8
ΔE_{def}^{SCF}	−187.7	−310.3	−85.7	−156.5
$\epsilon_{ind}^{(20)}$	−309.5	−393.3	−114.8	−176.3
$\epsilon_{ind-r}^{(20)}$	−356.9	−452.6	−131.0	−201.4
$\epsilon_{es-r}^{(12)}$	−40.2	−47.4	−17.8	−11.1
$\epsilon_{disp}^{(20)}$	−972.5	−877.1	−582.6	−542.5
$\Delta E_{exch}^{(2)}$	146.4	140.7	71.6	76.9
$\epsilon_{disp}^{(21)}$	106.6	77.6	56.7	41.5
$\Delta E^{SCF}+\epsilon_{disp}^{(20)}$	−542.1	−561.6	−425.8	−430.8

TABLE IV. R and θ dependences of the ΔE^{SCF} and the total $\Delta E(2)$ interaction energies for Kr–NH_3; energies in μhartrees, R in a_0.

	$\chi=0.0°$									
θ	$R=7.0$		$R=7.5$		$R=8.0$		$R=9.0$		$R=10.0$	
(deg)	SCF	$\Delta E(2)$	SCF	$\Delta E(2)$	SCF	$\Delta E(2)$	SCF	$\Delta E(2)$	SCF	$\Delta E(2)$
180	···	···	614.2	−119.7	261.6	−258.5				
160	···	···	624.0	−139.3					2.6	−139.6
140	···	···	584.9	−229.2			31.1	−247.9	−0.6	−144.5
120	1164.2	−66.1	456.9	−374.3	172.6	−394.7	11.4	−256.3	−3.5	−143.2
100	826.2	−354.9	308.1	−482.9	109.1	−426.7	7.5	−248.8	−3.9	−134.9
80	621.5	−447.6	228.4	−491.2	79.5	−410.2	5.4	−231.4	−2.6	−124.9
60	607.5	−356.4	230.5	−426.6	83.3	−369.4				
40	695.3	−204.2	269.1	−351.0	97.5	−334.4				
0	···	···	312.2	−330.9	109.7	−311.1				
	$\chi=60.0°$									
	$R=7.5$		$R=8.0$		$R=8.5$		$R=9.0$		$R=10.0$	
140	777.1	−131.4	308.0	−317.5	115.7	−318.7	38.9	−265.6	−1.3	−156.3
120	857.8	−182.7	324.0	−374.1	113.5	−361.2	33.4	−293.9	−4.7	−167.5
100	731.9	−298.1	268.9	−415.9	90.6	−371.6	24.7	−292.3	−5.2	−162.2
80	491.6	−388.7	178.9	−412.6	59.9	−343.0	16.3	−262.3	−3.4	−143.5
40			108.9	−334.0						

hydrogen-bonding orientation were also noticed in our calculations for the complex between Ar and such a poor proton donor as CH_4.[12]

The partitioning of the interaction energy is shown in Table V. In contrast to the Ar–H_2O or Kr–H_2O cases, the decompositions at the two configurations, H-bonded and T, do not differ qualitatively. For instance, the SCF-deformation and induction effects are relatively small and unimportant for both geometries. One may conclude that Kr is as reluctant as Ar to form an H bond to ammonia. However, the T configuration minimum in the Kr–NH_3 case appears to be shifted slightly toward larger θ angles, thus indicating a more H-bond character.

TABLE V. Interaction energy contributions for Kr–NH_3 and Ar–NH_3 in the H-bonded and T geometries. The parameters in parentheses correspond to the (R,θ) values; all energies in μhartrees.

	Kr–NH_3		Ar–NH_3
	T (7.5 a_0, 80°)	H-bond (8.0 a_0, 100°)	T (7.1 a_0, 80°)
ΔE^{SCF}	228.4	268.9	252.5
$\Delta E^{(2)}$	−719.6	−684.8	−667.2
$\Delta E(2)$	−491.2	−415.9	−414.7
ϵ_{exch}^{HL}	415.7	491.2	437.8
$\epsilon_{es}^{(10)}$	−129.8	−123.3	−132.9
ΔE_{def}^{SCF}	−57.5	−99.0	−52.4
$\epsilon_{ind}^{(20)}$	−140.0	−164.3	−126.4
$\epsilon_{ind-r}^{(20)}$	−158.2	−188.1	···
$\epsilon_{es-r}^{(12)}$	−32.8	−26.9	−33.2[a]
$\epsilon_{disp}^{(20)}$	−802.2	−748.9	−757.0
$\Delta E_{exch}^{(2)}$	115.4	91.0	123.0
$\epsilon_{disp}^{(21)}$	96.9	66.4	···
$\Delta E^{SCF}+\epsilon_{disp}^{(20)}$	−573.8	−480.0	−504.5

[a]This value corresponds to $\epsilon_{es}^{(12)}$.

IV. CONCLUSIONS

A. Comparison of Kr–H_2O and Kr–NH_3

In search for factors which would characterize possible differences/similarities between the properties of NH_3 and H_2O pertaining to the ability of formation of the H-bonded structures we focus on the two dominant attractive contributions SCF deformation and dispersion.

The dispersion contribution is an entirely electronic contribution in the sense that it is not directly related to the charges and positions of the nuclei. Indeed, the dispersion energy is an electron correlation effect and its expression includes only the two-electron integrals. Considering the X-H–Y hydrogen-bond interaction, the dispersion energy will be the smaller the more strongly electrons are shifted toward the X atom, i.e., the more is this bond polar. Therefore, the dispersion energy does not favor the H-bonded structures.

On the other hand, the induction and the SCF-deformation contributions reflect the electric polarization caused by both the electron charge cloud and the charges on nuclei. Consequently, in the X-H–Y interaction the effects will be the larger the more electrons are shifted toward X, i.e., the more polar the X–H bond gets. Therefore, the induction and SCF-deformation effects favor the H-bond structure.

In the atom–molecule interactions involving closed-shell species, the interplay between these two effects, the dispersion and SCF deformation, may be well characterized by analyzing the ratio of these two contributions, $\Delta E_{def}^{SCF}/\epsilon_{disp}^{(20)}$. The maxima of this ratio should help indicate the regions of PES which are particularly active in the induction interaction. It should be added that the electrostatic term (although quantitatively non-negligible) which in these complexes originates from charge-overlap effects is

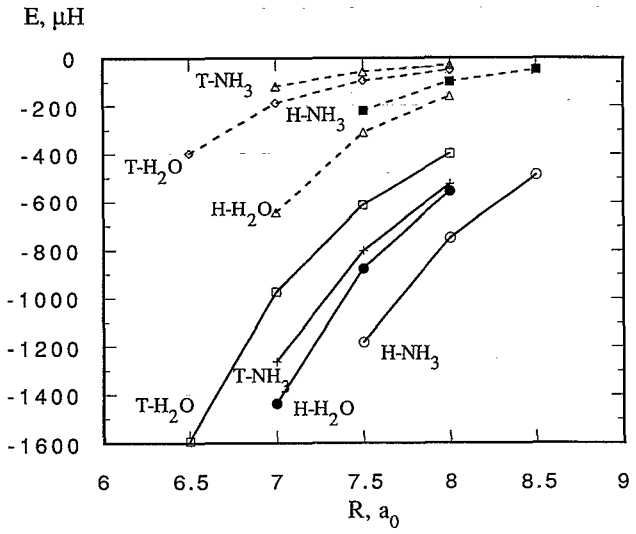

FIG. 2. R dependence of the SCF deformation (dashed line) and dispersion (solid line) energies for Kr–H_2O and Kr–NH_3. The following abbreviations have been used: "T-NH_3"–Kr-NH_3 at $\theta=80°$, $\chi=0°$; "H-NH_3"–Kr-NH_3 at $\theta=100°$, $\chi=60°$; "T-H_2O"–Kr-H_2O at $\theta=80°$, $\chi=0°$; "H-H_2O"–Kr-H_2O at $\theta=120°$, $\chi=0°$.

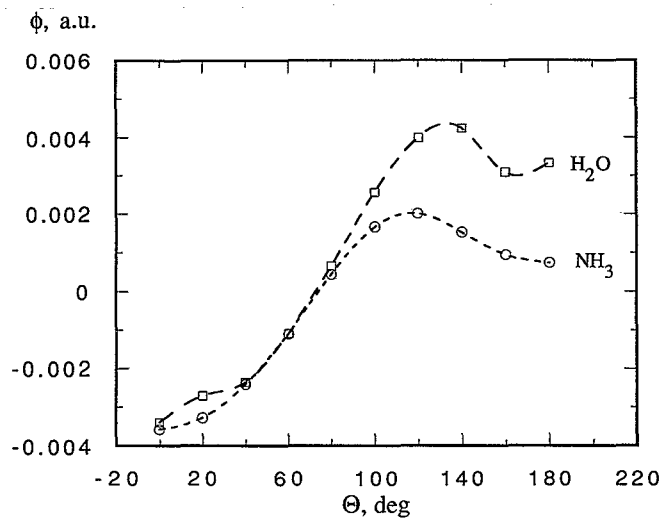

FIG. 4. θ dependence of the electric field (ϕ) at the position of Kr around H_2O ($R=7.5\ a_0$) and NH_3 ($R=8.0\ a_0$). The values shown are the projection of the field vector on the O(N)–Kr axes.

of secondary importance as far as the anisotropy is concerned.

To illustrate this point the dispersion and SCF-deformation energies are plotted in Fig. 2 for Kr–NH_3 and Kr–H_2O complexes. The comparison of the H-bonded configurations of both complexes indicates that Kr–NH_3 has larger dispersion and smaller SCF-deformation energies than Kr–H_2O (see Fig. 2). This means that electrons in the O–H bond are shifted more strongly toward the heavy atom than those in the N–H bond. In other words, the O–H bond may be viewed as more polar.

The θ dependence of the ratios $\Delta E_{\rm def}^{\rm SCF}/\epsilon_{\rm disp}^{(20)}$ (def/disp) plotted in Fig. 3 leads to further interesting conclusions. The three curves correspond to the R distances of the minimum for Kr–H_2O ($R=7.5\ a_0$), the minimum for Kr–NH_3 ($R=7.5\ a_0$), and of the saddle point at the H-bond configuration for Kr–NH_3 ($R=8.0\ a_0$). The ratios def/disp have maxima at the heavy-atom ends ($\theta=0.0°$), as well as at the hydrogen ends ($\theta=100$–$120°$). The region of the T configuration for Kr–NH_3 (80°–100°) is very flat with a tiny flat maximum around the H–H edge of ammonia. It is seen that all the three heavy-atom maxima are very close in magnitude. The maxima at the H ends, on the other hand, differ markedly. In the NH_3 case the H maximum is much lower than the N maximum, whereas in the case of H_2O the H maximum is much higher than that at the O end. This behavior strongly suggests that the O–H bond and the N–H bond are intrinsically different in their ability to form H bonding. By virtue of maximizing the def/disp ratio the former can be considered H-bond active while the latter cannot.

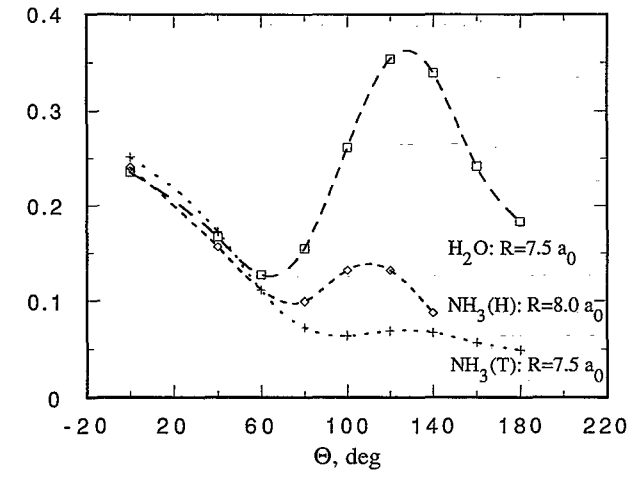

FIG. 3. θ dependence of the ratio $\Delta E_{\rm def}^{\rm SCF}/\epsilon_{\rm disp}^{(20)}$ for Kr–H_2O and Kr–NH_3. "T" corresponds to $\chi=0.0°$, "H" corresponds to $\chi=60°$.

The results of Fig. 3 lead us to the conclusion that the regions around N and O, as well as the H of H_2O, are capable of maximizing the electrostatic and induction interactions, whereas the region around the H of NH_3 is not. To confirm this observation the magnitude of the electric field in the position of Rg as a function of the angle θ is plotted in Fig. 4. A large electric field is seen at both heavy atoms and at the H ends of water. The electric field at the H end in NH_3 is much smaller. Consequently, the O and H ends in H_2O, as well as the N end in NH_3, are expected to strongly attract ions, polar molecules, as well as highly polarizable species. Several known structures of van der Waals complexes involving water confirm this conclusion, namely H_2O–Na^+,[38] H_2O–Cl^-,[39] CH_4–H_2O,[40] H_2–H_2O.[41] On the other hand, it is also known that for complexes where the electrostatic and induction interactions are quite small, the directions of approach to water and ammonia are those which minimize the exchange repulsion, that is, the T configurations [examples: He–H_2O,[18] H–H_2O,[42] Ar–NH_3 (Ref. 8)]. An intermediate situation is observed in

$Ar–H_2O$,[11] whose broad minimum encompasses both types of situations.

ACKNOWLEDGMENTS

This work was supported by the National Institutes of Health (Grant No. GM36912) and by the Polish Committee for Scientific Research KBN Grant No. 2 0556 91 01. We wish to thank Professor A. van der Avoird for making available to us results of Ref. 3 prior to publication, and to Dr. C. A. Schmuttenmaer for sending us a copy of his Ph.D. thesis.

[1] C. A. Schmuttenmaer, R. C. Cohen, J. G. Loeser, and R. J. Saykally, J. Chem. Phys. **95**, 9 (1991).
[2] I. I. Suni, S. Lee, and W. Klemperer, J. Phys. Chem. **95**, 2859 (1991).
[3] J. G. Loeser, C. A. Schmuttenmaer, R. C. Cohen, M. J. Elrod, D. E. Steyert, R. J. Saykally, R. E. Bumgarner, and G. A. Blake, J. Chem. Phys. **97**, 4727 (1992); J. W. I. van Bladel, A. van der Avoird, P. E. S. Wormer, and R. J. Saykally, *ibid.* **97**, 4750 (1992).
[4] D. D. Nelson, W. Klemperer, G. T. Fraser, F. J. Lovas, and R. D. Suenram, J. Chem. Phys. **87**, 6364 (1987); D. D. Nelson, G. T. Fraser, and W. Klemperer, *ibid.* **83**, 6201 (1985).
[5] G. T. Fraser, D. D. Nelson, Jr., A. C. Charo, and W. Klemperer, J. Chem. Phys. **82**, 2535 (1985).
[6] D. D. Nelson, G. T. Fraser, K. I. Peterson, K. Zhao, W. Klemperer, F. J. Lovas, and R. D. Suernam, J. Chem. Phys. **85**, 5512 (1986).
[7] D. H. Gwo, M. Havenith, K. L. Busarow, R. C. Cohen, C. A. Schmuttenmaer, and R. J. Saykally, Mol. Phys. **71**, 453 (1990).
[8] G. Chałasiński, S. M. Cybulski, M. M. Szczęśniak, and S. Scheiner, J. Chem. Phys. **91**, 7809 (1989).
[9] J. W. I. van Bladel, A. van der Avoird, and P. E. S. Wormer, J. Chem. Phys. **94**, 501 (1991).
[10] M. Bulski, P. E. S. Wormer, and A. van der Avoird, J. Chem. Phys. **94**, 491 (1991).
[11] G. Chałasiński, M. M. Szczęśniak, and S. Scheiner, J. Chem. Phys. **94**, 2807 (1991).
[12] M. M. Szczęśniak, G. Chałasiński, and S. M. Cybulski, J. Chem. Phys. **96**, 463 (1992).
[13] G. Chałasiński, M. M. Szczęśniak, and B. Kukawska-Tarnawska, J. Chem. Phys. **94**, 6677 (1991).
[14] G. Chałasiński and M. M. Szczęśniak, Croat. Chim. Acta (in press).
[15] J. M. Hutson, Annu. Rev. Phys. Chem. **41**, 123 (1990).
[16] R. C. Cohen and R. J. Saykally, J. Phys. Chem. **94**, 7991 (1990); J. Chem. Phys. **95**, 7891 (1991).
[17] R. Viswanathan and T. R. Dyke, J. Chem. Phys. **82**, 1674 (1985).
[18] A. Palma, S. Green, D. J. DeFrees, and A. D. McLean, J. Chem. Phys. **89**, 1401 (1988); S. Green, D. J. DeFrees, and A. D. McLean, *ibid.* **94**, 1346 (1991).
[19] S. Rybak, B. Jeziorski, and K. Szalewicz, J. Chem. Phys. **95**, 6576 (1991).
[20] G. Chałasiński and M. M. Szczęśniak, Mol. Phys. **63**, 205 (1988).
[21] R. Moszyński, S. Rybak, S. M. Cybulski, and G. Chałasiński, Chem. Phys. Lett. **166**, 609 (1990); S. M. Cybulski, G. Chałasiński, and R. Moszyński, J. Chem. Phys. **92**, 4357 (1990).
[22] M. Gutowski and L. Piela, Mol. Phys. **64**, 943 (1988).
[23] M. Jeziorska, B. Jeziorski, and J. Čížek, Int. J. Quantum. Chem. **32**, 149 (1987).
[24] M. Gutowski, F. B. van Duijneveldt, G. Chałasiński, and L. Piela, Mol. Phys. **61**, 233 (1987); Chem. Phys. Lett. **129**, 325 (1986).
[25] M. Gutowski, J. H. van Lenthe, J. Verbeek, F. B. van Duijneveldt, and G. Chałasiński, Chem. Phys. Lett. **124**, 370 (1886).
[26] J. H. van Lenthe, J. G. C. M. van Duijneveldt-van de Rijdt, and F. B. van Duijneveldt, Adv. Chem. Phys. **69**, 521 (1987).
[27] G. Chałasiński and M. Gutowski, Chem. Rev. **88**, 943 (1988).
[28] M. M. Szczęśniak and S. Scheiner, J. Chem. Phys. **84**, 6328 (1986).
[29] S. F. Boys and F. Bernardi, Mol. Phys. **19**, 553 (1970).
[30] B. Jeziorski and M. van Hemert, Mol. Phys. **31**, 713 (1976).
[31] A. J. Sadlej, Coll. Czech. Chem. Commun. **53**, 1995 (1988).
[32] S. Huzinaga, M. Kłobukowski, and H Tatewaki, Can. J. Chem. **63**, 1812 (1985).
[33] J. Andzelm, S. Huzinaga, M. Kłobukowski, and E. Radzio, Mol. Phys. **52**, 1495 (1984).
[34] GAUSSIAN 88, M. J. Frisch, M. Head-Gordon, H. B. Schlegel, K. Raghavachari, J. S. Binkley, C. Gonzales, D. J. Defrees, D. J. Fox, R. A. Whiteside, R. Seeger, C. F. Melius, J. Baker, R. L. Martin, L. R. Kahn, J. J. P. Stewart, E. M. Fluder, S. Topiol, and J. A. Pople, Gaussian Inc., Pittsburgh, PA, 1988.
[35] GAUSSIAN 90, M. J. Frisch, M. Head-Gordon, G. W. Trucks, J. B. Foresman, H. B. Schlegel, K. Raghavachari, M. A. Robb, J. S. Binkley, C. Gonzales, D. J. Defrees, D. J. Fox, R. A. Whiteside, R. Seeger, C. F. Melius, J. Baker, R. L. Martin, L. R. Kahn, J. J. P. Stewart, S. Topiol, and J. A. Pople, Gaussian, Inc., Pittsburgh, PA, 1990.
[36] S. M. Cybulski, Trurl package, Carbondale, IL, 1990.
[37] R. C. Cohen and R. J. Saykally, J. Phys. Chem. **96**, 1024 (1992); C. A. Schmuttenmaer, Ph.D. dissertation, University of California, Berkeley, 1991.
[38] C. W. Bauschlicher, S. R. Langhoff, H. Partridge, J. E. Rice, and A. Komornicki, J. Chem. Phys. **95**, 5142 (1991).
[39] J. E. Del Bene, Struct. Chem. **1**, 19 (1989).
[40] M. M. Szczęśniak, G. Chałasiński, S. M. Cybulski, and P. Cieplak (unpublished).
[41] Q. Zhang, L. Chenyang, Y. Ma, F. Fish, M. M. Szczęśniak, and V. Buch, J. Chem. Phys. **96**, 6039 (1992).
[42] Q. Zhang, N. Sabelli, and V. Buch, J. Chem. Phys. **95**, 1080 (1991).